Astron. Astrophys. 335, 161–172 (1998)

ASTRONOMY AND ASTROPHYSICS

High-energy gamma-ray emission from the Galactic Center

H.A. Mayer-Hasselwander[1], D.L. Bertsch[2], B.L. Dingus[3], A. Eckart[1], J.A. Esposito[2,10], R. Genzel[1], R.C. Hartman[2], S.D. Hunter[2], G. Kanbach[1], D.A. Kniffen[4], Y.C. Lin[5], P.F. Michelson[5], A. Mücke[1], C. von Montigny[6], R. Mukherjee[7], P.L. Nolan[5], M. Pohl[8], O. Reimer[1], E.J. Schneid[9], P. Sreekumar[2,10], and D.J. Thompson[2]

[1] Max-Planck-Institut für Extraterrestrische Physik, D-85748 Garching, Germany
[2] NASA Goddard Space Flight Center, Greenbelt, MD 20771, USA
[3] University of Utah, Salt Lake City, Utah, USA
[4] Department of Physics and Astronomy, Hampden-Sydney College, Hampden-Sydney, VA 23943, USA
[5] W.W. Hansen Experimental Physics Laboratory and Department of Physics, Stanford University, Stanford, CA 94305, USA
[6] Landessternwarte Königstuhl, D-69117 Heidelberg, Germany
[7] Barnard College & Columbia University, Columbia Astrophysics Lab, New York, NY 10027, USA
[8] Danish Space Research Institute, DK-2100 Copenhagen O, Denmark
[9] Northrop Grumman Corporation, Bethpage, NY 11714, USA
[10] USRA Research Associate

Received 24 September 1997 / Accepted 24 March 1998

Abstract. The EGRET instrument on the Compton Gamma-Ray Observatory has observed the Galactic Center (GC) region with good coverage at a number of epochs. A strong excess of emission is observed, peaking at energies > 500 MeV in an error circle of 0.2 degree radius including the position $l = 0°$ and $b = 0°$. The close coincidence of this excess with the GC direction and the fact that it is the strongest emission maximum within 15 degrees from the GC is taken as compelling evidence for the source's location in the GC region. The history of the emission intensity, observed over 5 years, leaves room for possible time variation; however, it does not provide evidence. The angular extent of the excess appears only marginally compatible with the signature expected for a single compact object. The emission therefore may stem from one or more compact objects or may originate from diffuse interactions within 85 pc from the center of the Galaxy at 8.5 kpc distance. The spatial distribution of the emission does not correlate with the details of the CO-line surveys. Thus, in spite of the existence of a strong emission peak, earlier conclusions based on an apparent 'gamma-ray deficit', postulating the masses of the 'wide-line' clouds in the GC area to be an order of magnitude lower than indicated by naive CO interpretation, are supported. However, the total gas mass in the Nuclear Bulge (NB) derived from the gamma-ray emission is found to be in agreement with the mass which in recent studies has been derived from molecular-line and FIR surveys. The γ-ray emission spectrum is peculiar and different from the spectrum of the large-scale galactic diffuse emission. A diffuse emission scenario requires an enhanced and peculiar Cosmic Ray (CR) spectrum as suggested for the electrons in the 'Radio Arc'. A compact sources model hints at an origin in pulsars. While the spectrum suggests middle-aged pulsars like Vela, too many are required to produce the observed flux. The only detected very young pulsar, the Crab pulsar, has an incompatible spectrum. However, it is not proven that the Crab spectrum is characteristic for all young pulsars: thus, a single or a few very young pulsars (at the GC not detectable in radio emission), provided their gamma-ray emission is larger than that of the Crab pulsar by a factor of 13, are likely candidates. Alternatively, more exotic scenarios, related to the postulated central black hole or dark matter (neutralino) annihilation, may be invoked.

Key words: ISM: clouds – ISM: general – Galaxy: center – gamma rays: observations

Send offprint requests to: HRM@MPE.MPG.DE

1. Introduction

Gamma-ray emission from the Galactic Disk in the 30 MeV to 30 GeV range has been observed by the telescopes on the OSO-3, SAS-2, COS-B spacecrafts and lately by the EGRET telescope on the Compton Gamma-Ray Observatory (CGRO). The comparison of the observed emission with models for interaction of galactic Cosmic Rays (CRs) with interstellar matter (Strong 1995; Hunter et al. 1997) has confirmed the expectation that a large fraction of the Galaxy's gamma-ray emission stems from large-scale diffuse collision processes. The emissivity at a particular location usually is proportional to the product of target-particle (atoms, photons) density and CR (nucleons, electrons) density. The distribution of the emission as recorded by the observing instruments is determined by its actual spatial distribution within the Galaxy (intensity, direction, distance) and also by the angular resolution of the observing telescopes. An emission excess from the Galactic Center (GC) at 8.5 kpc distance needs to be resolved within the intense and narrow band of foreground- and background emission from the large-scale

Galactic Disk. With current or previous instruments it only will be detectable if either the target-particle density or the CR density or both are peaking sharply within a few hundred pc from the GC. The galactic CO-line survey (Dame et al. 1987), which throughout the Galaxy had been found to be a good tracer for interstellar molecular gas, shows a strong and structured excess originating from within the Nuclear Bulge (NB) which extends over the innermost 300 pc in radius. Postulating the CR density within the NB to be not significantly lower than the average derived for a galactocentric radius < 5 kpc, led to the expectation that a strong and structured gamma-ray-emission excess should be observed, originating from interaction of CRs with the massive molecular clouds, located within the NB as indicated by the CO-line survey.

It was an astonishing result of the COS-B mission that no pronounced source excess was observed in the direction to the GC. It was shown by Blitz et al. (1985), that the absence of a corresponding strong gamma-ray peak implies that in the volume surrounding the GC within a few hundred parsecs the H_2 to ^{12}CO ratio is most likely smaller by an order of magnitude than elsewhere in the Galaxy. This can be understood when investigating the CO surveys in more detail: the CO-line emission in the neighbourhood of the GC shows high velocity and velocity dispersion, not related to the galactic rotation. This atypical emission is attributed to gas clouds in local orbital motion and high turbulence. The clouds also are expected to be under extreme conditions like high tidal forces and temperatures. This causes the highly velocity-dispersed CO emission to be observed optically much thinner, making the usual conversion factor to H_2 irrelevant (Stacy et al. 1987; Stark et al. 1991). The presumably increased metallicity in the relevant volume also suggests a much lower H_2 to ^{12}CO ratio. Therefore the gas tracing molecular-line surveys, when naively interpreted, indicate far too much gas and are of no value for a gas mass estimate within 3 degrees longitude from the GC. Further, at $l = 0^\circ$ no reliable information is obtainable for the amount of HI by 21 cm observations due to the lack of sufficient galactic-rotation velocity and velocity-dispersion in the direction of the line-of-sight. In addition, strong self-absorption does affect the foreground- and background emission. Therefore, the amount of HI possibly concentrated within 100 pc from the GC is relatively unknown. Recent far-infrared (FIR) observations by the Diffuse Infrared Background Experiment (DIRBE) on COBE (Sodroski et al. 1994) show a less pronounced and more narrow spike in the longitude profile through the GC compared to CO. The comparison of the CO and FIR surveys therefore indicate that the ^{12}CO to dust ratio is unusually high and also that the emission from dust appears to originate from a smaller volume around the GC. The indicated uncertainties in the gas to dust ratio and other complications of the dust-tracing FIR emission (temperature) also tend to overestimate the gas mass in the central region.

Sodroski concluded that the gas mass is probably less than required to be observable in gamma-rays by COS-B, which according to Blitz et al. (1985) gave a surprisingly low upper limit of 4×10^{-7} photons cm^{-2} s^{-1} for a point-source at the GC and energies > 300 MeV. We have reinvestigated the COS-B data by comparing the > 300 MeV intensity profile given in Mayer-Hasselwander et al. (1982) with the corresponding EGRET intensity profile and find fully compatible excesses for both profiles within 3 degrees longitude from the GC. We cannot reconstruct the COS-B result from Blitz et al. (1985): it appears too low by at least a factor 2.5. According to our analysis of COS-B and EGRET data, a correspondingly higher GC source flux on top of the predicted large-scale-galactic diffuse emission (Hunter et al. 1997) can be accommodated and thus the observed gamma-ray emission constrains the amount of diffuse emission from the GC less than do the FIR observations.

As previous COS-B analyses did not indicate a 'localised' source excess and gas mass estimates had been reduced also on other arguments, it again was an unexpected result that EGRET found a pronounced source excess at the GC position (Mayer-Hasselwander et al. 1992, 1993) which is designated in the second EGRET catalog (Thompson et al. 1995) by 2EG J1746-2852. The EGRET detection of a source at the GC is based on energies above 100 MeV; the location of the source is best determined in the energy ranges above 500 MeV and there is found perfectly compatible with the GC (Lamb & Macomb 1997, Reimer et al. 1997). The high-energy gamma-ray measurements by EGRET are of great importance for the understanding of the innermost part of our Galaxy at several scales within 1 kpc. It is evident that narrowing down the range of possible scenarios by demonstrating either stability or variability of the emission, by confining the extent and location of the source and by determining the source spectrum in detail is essential for the scientific value of this unexpected EGRET discovery.

It is the topic of this paper to present the observational details and to derive the constraints which the EGRET observations put on the nature of the source excess in the GC. The GC source had to be considered as possibly extended and confused and embedded in high and structured background; this required the application of analysis procedures partially different from those used in EGRET standard analyses.

2. Data and analysis

2.1. EGRET data

EGRET gamma-ray data relevant for the analysis of the GC region from observation cycles 1, 2, 3, 4 and part of 5 are used. Table 1 lists the observation periods and their parameters. For the purpose of time variation analysis short observations at neighbouring epochs were grouped into clusters and were combined in order to get statistically significant results. For the purpose of structural and spectral investigations the data from all observations were added.

The analysis started with the standard EGRET calibration and exposures files. The latter contain sensitivity corrections for each viewing period. These corrections to exposures for individual observation periods in each energy range were derived (Esposito et al. 1998) in order to account for in-flight variation of sensitivity, primarily caused by the intrinsic ageing of the spark-chamber gas. In this procedure, regions dominated by diffuse

Table 1. Observation period parameters

Observ. Period Number	Start Day MJD	End Day MJD	Duration days	Pointing Direction Longit. deg	Pointing Direction Latitude deg	Gal Center Offset deg	Combined Dataset Name	Center Epoch MJD	Duration days	Aver. Offset deg	Exposure 300-1000 cm**2 s
50	48449,8	48463,8	14,0	0,0	-4,0	4,0	A	48456	14,0	4	5,00E+08
160	48602,8	48617,7	14,9	0,0	20,3	20,3	B	48609	14,9	20	2,85E+08
2100	49040,7	49043,5	2,8	355,6	6,3	7,7	C	49103	19,9	7	3,44E+08
2140	49075,7	49078,6	2,9	355,6	6,3	7,7	C				
2190	49112,7	49113,9	1,2	350,1	15,9	18,6	C				
2230	49138,6	49141,6	3,0	359,1	-0,1	0,9	C				
2260	49157,6	49167,5	9,9	355,0	5,0	7,1	C				
2290	49209,6	49210,7	1,0	5,0	5,0	7,1	D	49230	31,7	10	4,30E+08
2295	49211,7	49216,5	4,8	5,0	5,0	7,1	D				
2320	49223,6	49237,6	13,9	347,5	0,0	12,5	D				
3023	49239,7	49251,6	11,9	1,4	9,3	9,4	D				
3230	49433,7	49447,6	13,9	356,8	-11,3	11,7	E	49450	20,7	13	3,47E+08
3240	49461,7	49468,5	6,8	15,0	5,6	16,0	E				
3300	49513,6	49517,6	3,9	18,0	0,0	18,0	F	49543	33,0	17	4,58E+08
3320	49521,6	49538,6	17,0	18,0	0,0	18,0	F				
3340	49551,6	49558,5	6,9	9,0	-8,4	12,3	F				
3365	49568,6	49573,9	5,3	340,4	2,9	19,8	F				
4210	49874,8	49881,5	6,8	355,3	0,4	4,7	G	49891	33,5	6	4,10E+08
4220	49881,6	49888,7	7,0	355,4	-0,4	4,6	G				
4230	49888,8	49898,6	9,8	2,6	-0,2	2,6	G				
4235	49898,7	49908,5	9,9	345,7	13,5	19,5	G				
4290	49980,6	49987,6	7,0	18,3	4,0	18,8	H	49984	7,0	19	6,14E+07
5080	50065,7	50071,6	5,9	6,5	-0,2	6,5	I	50068	5,9	7 (N)	9,65E+07
5161	50160,7	50163,6	2,9	341,1	5,6	19,7	K	50246	12,8	17 (N)	4,49E+07
5295	50322,7	50332,6	9,9	345,0	2,5	15,2	K				

MJD=JD-2400000.5; Average Offset = Exposure weight. Angle GC to Instrument Axis; N = Narrow Field of View;

(and therefore non-variable) emission, that were observed in more than one observation at different epochs, were compared. The standard corrections were derived to normalise the average intensity for the whole field of view of an observation period to observations when the sparkchamber performance was close to its originally-calibrated level. This normalisation postulates smooth variation versus epoch, i.e. no significant changes in performance on short timescales, except when a gas change took place. On a large scale, this correction procedure provides a good fit to the instrument performance.

For a particular direction in the sky, some additional irregular sensitivity variations are seen. Because the GC is a particularly complicated and interesting region, additional constraints and corrections for in-flight effects beyond the standard corrections were applied:

1. Only gamma rays incident within 25 degrees from the instrument pointing direction were accepted, in order to minimise source to instrument-axis offset-angle effects. The standard EGRET analysis extends to 30 degrees.
2. For each GC observation and for each energy range, additional correction factors were derived on the basis of the non-variable, intense galactic diffuse emission observed from directions less than 20 degree from the GC direction. Essentially, the data from each observation period were normalised in such a way that the normalisation is optimum for the GC location. For energies greater than 100 MeV these additional corrections in most cases are less than 15 percent. At lower energies in a very few cases in phase 4 and 5 data do these corrections reach a factor of 2; however, these observations have relatively low exposures and correspondingly low statistical weights in the analysis and thus their uncertainties do not affect the results.

2.2. Diffuse background model

The galactic-diffuse-emission model developed by Bertsch et al. (1993) and Hunter et al. (1994, 1995, 1997) is used to account for the large-scale galactic diffuse emission within which the GC source is embedded.

This model is based on ^{12}CO-line and HI surveys, a gas-coupled CR distribution model, and an inverse-Compton-emission model. Within 1 deg from $l = 0°$, where the HI tracer measurements are incorrect due to strong self-absorption and optical thickness effects (no velocity dispersion), the HI data were interpolated. In the range 354 to 10 degrees longitude the model disregards untypical high-velocity ^{12}CO emission which is observed from the NB cloud complexes. Low velocity emission, tracing the intercloud medium and also low velocity emis-

Table 2. Diffuse background model parameters

Diffuse Emission Model Parameters, for |l|, |b| < 20°			
Energy		Local Fit	
#	Range	Flat Component	Emissivity / H-atom
	MeV	ph cm^{-2} s^{-1} sr^{-1}	Factor
1	30 - 50	3,40E-05	0,74
2	50 -70	1,59E-05	0,79
3	70 - 100	1,29E-05	0,77
4	100 - 150	1,08E-05	0,79
5	150 - 300	1,21E-05	0,78
6	300 - 500	5,50E-06	0,77
7	500 - 1000	4,50E-06	0,85
8	1000-2000	2,30E-06	1,05
9	2000-4000	1,00E-06	1,28
10	4000 - 10000	4,00E-07	1,15

sion from the clouds is entering the model as observed. Therefore, the cloud complexes within 300 pc from the GC are not explicitly represented by the model. If emitting at a detectable level, they are expected to be visible as gamma-ray excesses exceeding the diffuse model. Depending on their location, several clouds would be visible as individually resolved sources and others would contribute to an extended source excess.

The EGRET data are well represented by the diffuse emission model plus an isotropic component (Sreekumar et al. 1997) on a galactic scale. At specific locations, however, deviations are observed. Therefore, in individual smaller regions the representation can be improved for the purpose of background estimation by additional local tuning in amplitude and bias. In standard EGRET analysis this tuning is implicit to the likelihood analysis algorithm 'LIKE' (Mattox et al. 1996). In this analysis the tuning was done as follows:

1. The model was tuned in each energy range to fit the gamma-ray data best in the region within 20 degrees from the GC. The constraint placed on the tuning procedure was that the data could not be exceeded by the model, such that the model forms a 'lower envelope', representing the diffuse emission, on which the emission excesses from individual sources are superimposed.
2. The galactic diffuse spectrum is known to be smooth. Thus, the tuning of the model has been iterated for each energy range, aiming to make the spectrum of the background model smooth (see Fig. 4). This procedure minimised the statistical scatter of the fit for each energy range.

Table 2 lists the tuning parameters applied to the EGRET diffuse model. The intense diffuse emission surrounding the GC region was therefore used as a fixed reference for both the normalisation (Sect. 2.1) and the background against which the GC region is viewed. This procedure removed much of the ambiguity that otherwise affects analysis in this complicated region. The tuned diffuse model was then used as a constant background in the timevariation- and spectral-analysis and as the reference for comparison of the derived GC source-spectrum with the spectrum of the diffuse emission.

2.3. Analysis

The analysis of a tentative source at the GC is difficult because a very distant galactic location is observed within the high background due to the galactic diffuse emission accumulating along the long line of sight in front of and beyond the GC.

Due to the limited angular resolution of the instrument, source confusion is a concern particularly at lower energies where the point spread function (PSF) extends over several degrees. The identification of the GC source as a single compact object therefore is possible only if variability is observed. If a spectrum distinctly different from that of the diffuse background emission is observed, then at least it can be demonstrated that the emission originates from a collection of peculiar sources or in an unusual diffuse emission scenario. We address these topics, along with the source significance, its possible extent, and its location, using the following methods:

1. The source location and significance is determined in four broad energy bands, 30–100, 100–300, 300–1000 and > 1000 MeV, accounting for the modelled diffuse background and using likelihood techniques.
2. The extent of the GC excess has been compared, on the basis of maps with 0.1 degree binning, with the extent of the source excesses observed for the three strongest pulsars: Vela, Geminga and Crab, which define the in-flight PSF. This analysis uses only the data above 1 GeV where the PSF is sharpest.
3. For the analysis of possible time variation, many observation periods distributed over several years had to be analysed individually. To obtain sufficient statistics for investigation of time-variability, three relatively wide energy bands were used: 100–300, 300–1000 and > 1000 MeV. For the time-variation analysis a forth energy band (30–100 MeV) is rather useless due to insufficient angular resolution with respect to the given background situation.
4. For the determination of the source spectrum, the counts from the GC source region have been analysed in 10 smaller energy bins from 30 MeV to 10 GeV by evaluating maps and profiles of counts and intensity directly as well as by using crosscorrelation- and likelihood-analysis (Hermsen 1980, Mattox et al. 1996) methods. Cross-calibrations between the different methods, especially with respect to in-flight uncertainties in the PSF, have been performed again for each energy range by comparison with the analysis of the 4 strongest pulsars (including PSR 1706-44). Finally the GC source-flux values in the low energy ranges were derived by likelihood analysis; in the energy ranges above 150 MeV the flux values were derived by a specific method of directly accumulating the source intensity within a small region (2 to 4 degree squares) of the binned data around the source, together with applying an energy dependent normalisation factor. This approach was found to be less sensitive to the problems of high, not-perfectly-modelled background. The errors are based on the values obtained in a likelihood analysis and were scaled in accordance to the ratio between the

source counts obtained in this specific analysis and in the likelihood analysis.

The method applied was the only available method allowing for source confusion and a finite source extent. It is to be noted, that the presence of a finite source extent or of an extended cluster of point sources can make the available EGRET standard point-source analysis algorithms (using likelihood or cross-correlation) inadequate because they are strictly based on the use of the PSF for counts representing a single point source only.

Source confusion is a severe limitation in the interpretation of the results. The space volume which might contribute unresolved sources to the observed excess increases drastically at lower energies due to the increasing size of the PSF. Thus the spectrum of a source at the GC location might be contaminated severely by additional soft sources located within degrees from the GC at energies below about 500 MeV. In this sense the observed spectrum of the GC source at energies below about 500 MeV represents an upper limit.

3. Results

3.1. Observational scenario and source significance

There are 5488 ± 516 counts observed for all energies above 30 MeV, representing the total source excess as seen by the analysis process described under 2.3. Illustrating the scenario, Fig. 1 displays residual counts maps, after subtraction of the model-predicted diffuse emission, in four energy ranges. Statistical fluctuations are only slightly smoothed, retaining all possibly significant structures in the maps. In addition to the evident GC excess two prominent sources, the pulsar PSR B1706-44 near $l = 343°, b = -3°$ and the quasar PKS 1622-297 near $l = 349°$, $b = 13°$, and several weaker sources are visible in the map. The number of counts observed for the sources are influenced by the exposure, which varies through the map. However, the relative fluxes in the four energy ranges seen for each of these sources already illustrate the fact that the GC excess and PSR B1706-44 have a much harder spectrum than the other sources.

3.2. Source extent

The extent of the GC excess has been compared, on the basis of maps with 0.1 degree binning and energies above 1 GeV where the angular resolution is best, with the extent of the source excesses observed for the pulsars: Vela, Geminga and Crab, which represent the in-flight PSFs. While the HWHM for the pulsars is 0.55 degree, the GC source excess has a HWHM of 0.7 degree. No established method is available to quantify the properties of a possibly extended source. We therefore estimate, using the in-flight PSF and gaussian function approximations, for the GC source a spatial intrinsic HWHM of 0.43 degree and a 68% flux enclosure angle of 0.6 degree. Thus, the bulk of emission from the GC source above 1 GeV is best compatible with emission originating at 8.5 kpc distance in a volume with a radius of 65 pc HWHM, respectively a volume with 85 pc radius for 68% containment. However, in view of uncertainties due to the high underlying intense and structured background, the source excess is still considered to be marginally compatible with emission from a single compact object. A two-component model (see Fig. 5), where the emission from a compact source region (60% from < 85 pc radius) is superimposed onto a resolved extended emission excess (40% from < 250 pc radius) is representing the data even better. Further, an extended source with 250 pc radius, for which the emissivity increases appropriately towards the center would have an indistiguishable appearance.

3.3. Source position

The positional analysis of the excess has been performed by cross-correlation and likelihood techniques, assuming a single point source. The position-error contours are given in Fig. 2 for several energy intervals above 100 MeV. Because there is evidence for extended emission from the source, the likelihood confinement contours are obtained too narrow, thus the discrepancy between the high and the low energy ranges becomes less significant. Still, the shift in the maximum supports the hypothesis that the emission below 300 MeV includes flux from one or several other objects located within 2 degrees from the GC. At these lower energies an unidentified soft source in the second EGRET catalog, 2EG J1747-3039 (Thompson et al. 1995), more recently designated as 3EG J1744-3011 with $l = 358.9, b = -0.5$ (Hartmann et al. 1998) may contribute. Several other objects in this region (GRO 1744-28, 2S1743-2941, E1740-2942, PSR1742-30, GRS1736-297, GRS 1739-278, GX359+02) might be considered as candidate counterparts, however, their spectra in energy ranges below gamma rays do not suggest their visibility in the high-energy gamma-ray regime.

The emission center at energies above 1 GeV is confined to the GC direction with a < 0.2 degree radius error box. This suggests that, at least at high energies, one source or extended emission volume with a very hard spectrum dominates the emission and is located or peaking within 30 pc from the actual GC. In light of the absence of other strong gamma-ray sources within 15 degrees of this direction, the statistical probability for this positional correlation to be a chance coincidence is about 10^{-4}, making it very likely that the source is located near the GC and not anywhere else along the line of sight.

3.4. Temporal characteristics

The 25 observation periods, some of which had only low exposure, were combined for time-variation analysis into 10 datasets (designated as A-K in Table 1 and Fig. 3). To minimise statistical uncertainties and at the same time keep spectral information and make use of good angular resolution at high energies, three energy ranges were used: 100–300 MeV, 300 MeV–1 GeV and > 1 GeV. The time history for the 3 energy ranges is displayed in Fig. 3. In addition to the flux values, also the applied sensitivity corrections, the (accordingly corrected) exposures and the observing angles of the source relative to the instrument axis are displayed. It is conspicuous that the points with the largest devia-

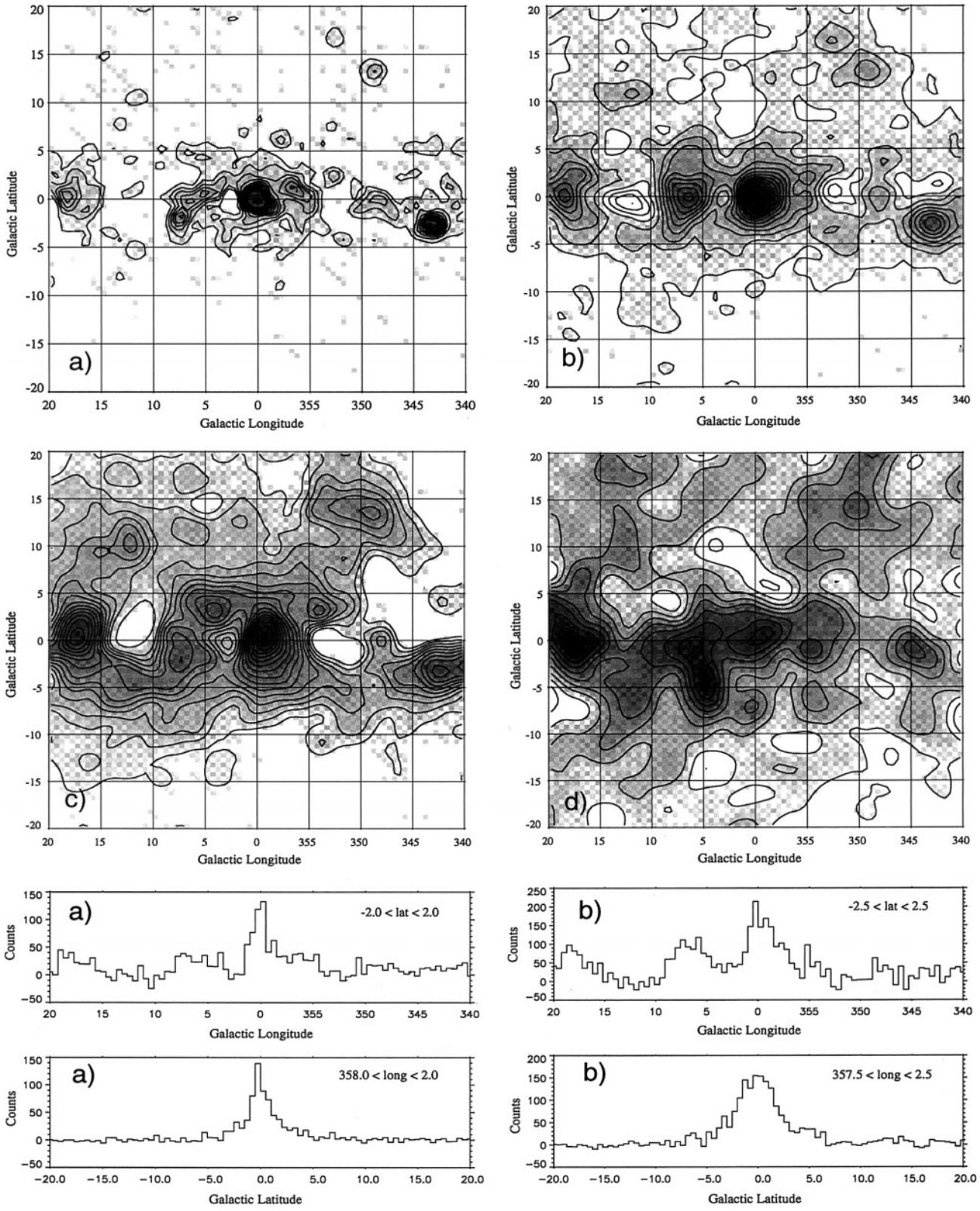

Fig. 1a–d Residual smoothed counts maps and profiles in several energy ranges after subtraction of the model-predicted diffuse emission background. The panels refer to these energy ranges: **a** $>$ 1 GeV, **b** 300 MeV–1 GeV, **c** 100–300 MeV, **d** 30–100 MeV.

tions from the linear regression line tend to have larger error bars and also the observational parameters are less favourable. This correlation suggests that there are residual uncorrected systematic effects. Even with no fine-tuning McLaughlin et al. (1996)

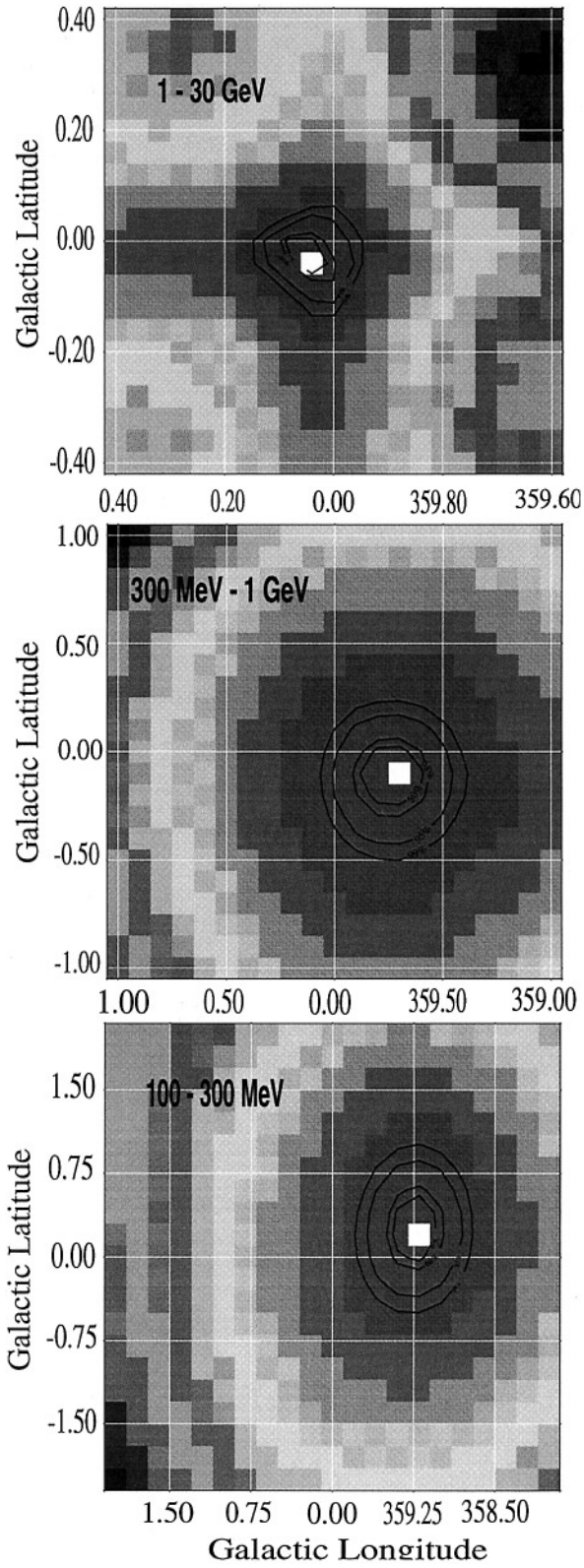

Fig. 2. The contour lines indicate the 50%, 68%, 95%, and 99% containment probability regions for the source position as derived by the EGRET likelihood analysis program.

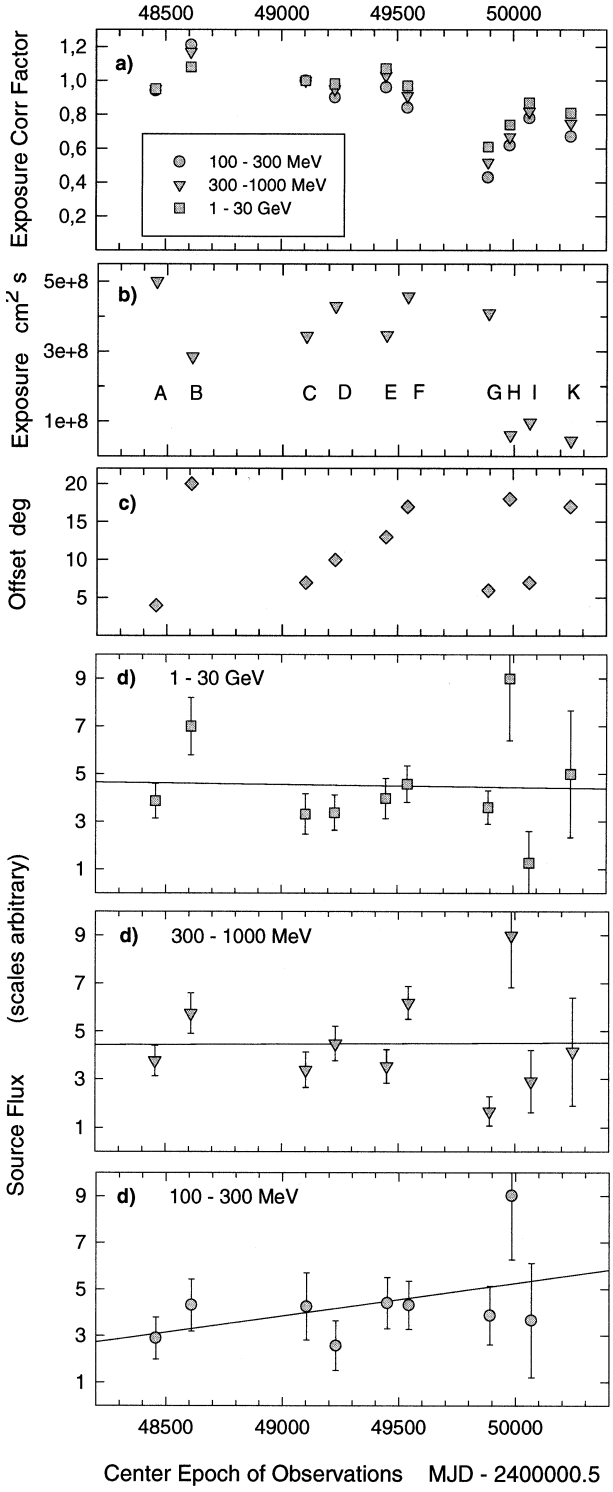

Fig. 3a–d Time history of the observed flux at ten epochs. Panel **a** displays the exposure correction factor which was applied to correct for in-flight sensitivity changes. Panel **b** gives the corrected exposure. Panel **c** shows the offset of the GC direction relative to the instrument axis. The panels **d** display the observed source fluxes in three energy ranges and corresponding linear regression lines. The data point for observation K at 100 to 300 MeV is out of range, it is a factor 2 larger in value and error than data point H, but is considered unreliable due to the short exposure and large offset angle.

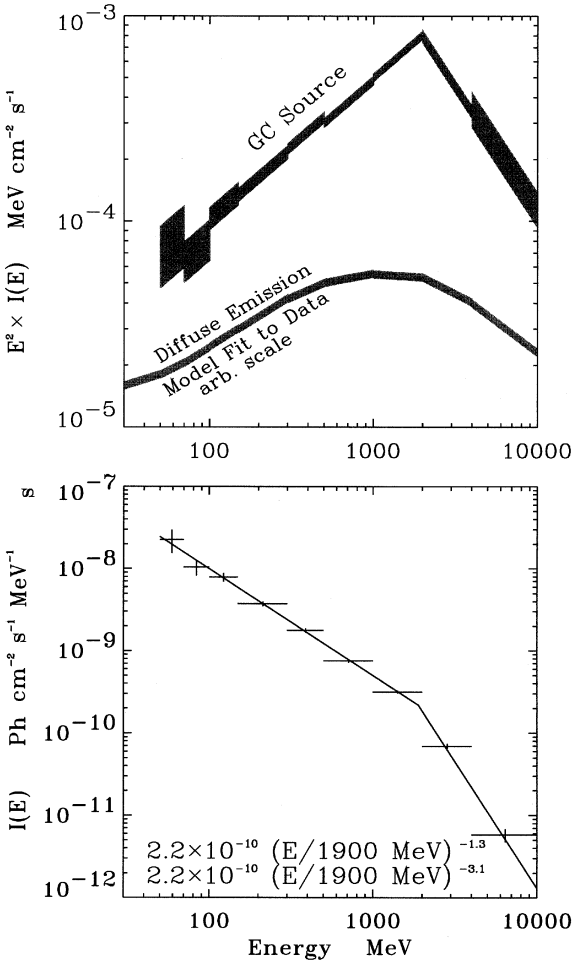

Fig. 4. The lower panel gives the differential photon spectrum for the GC source excess together with a broken-power-law fit. The upper panel shows the power (per ln(E) interval) spectrum for the source compared with the spectrum of the embedding galactic diffuse emission averaged in the longitude range 340–20 degrees.

found only weak evidence for variability of the GC source. With the present more careful treatment of this specific region, the indication for variability is even weaker. No long-term trend is seen, however, the possibility that a short term variation is indicated by observation B (or H), where the flux in all three energy ranges is above average, cannot be excluded.

A detailed reanalysis of the COS-B data, taken more than a decade earlier, was not feasible. However, the COS-B intensity profile given in Mayer-Hasselwander et al. (1982) for > 300 MeV has been compared with a directly corresponding EGRET profile and showed agreement for the intensity within 3 degrees longitude from the GC, when normalised on the disk intensities observed at 350 and 10 degree longitude. We conclude that there is no evident difference in the intensities which are observed on average during both missions. The lack of detection of a GC source by COS-B might be explained by differences in the background model used, together with COS-B's much lower sensitivity.

3.5. Energy spectrum

The emphasis in evaluation of the spectrum has been given to the question: is the spectral shape different from that expected from interactions of ambient CRs with the interstellar medium. The spectrum of the diffuse emission is derived from the diffuse model (Sect. 2.2) for the region within 20 degree in longitude and latitude from the GC. The spectra for the GC source and for the diffuse emission are compared in Fig. 4. They are seen to be distinctly different. It is interesting to note that, if neighbouring sources are involved at lower energies, being unresolved due to the broad PSF, then the true spectrum of the high energy source excess at $l = 0°$, $b = 0°$ will be harder and even more different from the diffuse emission spectrum. Previous analyses of the GC source spectrum by Fierro (1995) and Merck et al. (1996) were performed using EGRET standard analysis tools, presuming an unresolved point source. Those analyses already obtained rather hard spectra, somewhat different from the diffuse emission, however with a less pronounced peak and turnover at high energies. This much more detailed analysis clearly demonstrates that the spectrum of the GC source excess is not due to ambient CR-gas interaction. A very peculiar and very hard CR spectrum is required in order to explain the emission as diffuse processes.

Allowing for a total source-excess extent up to 1.5 degree in radius, the flux attributed to the source excess at $l = 0°$, $b = 0°$ is $(217 \pm 15) * 10^{-8}$ ph cm^{-2} s^{-1} for > 100 MeV corresponding to a luminosity of $(2.2 \pm 0.2) * 10^{37}$ erg s^{-1} for a source distance of 8.5 kpc. The fluxes in the energy bands are (in units of 10^{-8} ph cm^{-2} s^{-1}): (95±9) (100–300 MeV), (73±4) (300–1000 MeV), (49±3) (> 1 GeV).

The photon spectrum can be well represented by a broken power law with a break energy at 1900 MeV. Below this energy the differential photon spectrum is $F(E) = (2.2 \pm 0.01) * 10^{-10}(E/1900\,\mathrm{MeV})^{-1.30\pm0.03}$, above the break energy the spectrum is $F(E) = (2.2 \pm 0.01) * 10^{-10}(E/1900\,\mathrm{MeV})^{-3.1\pm0.2}$.

The fluxes and errors do not reflect systematic uncertainties concerning possible source confusion and limitations of the background model and background subtraction method. The likelihood of confusion with possible unresolved soft-spectrum sources in the neighbourhood of the GC increases to low energies: the observed spectrum, when allocated to the high-energy source at the GC position therefore must be considered to represent upper limits below ~ 300 MeV. In such a case an even harder spectrum is required for the central source.

The integral flux for the GC source (exceeding the modeled diffuse emission) in the energy range > 100 MeV in this analysis is obtained larger by a factor 2 than the value given for a point-source at the GC in the second EGRET catalog. The difference is due to the different analysis concepts: Here allowance is made for an extended source and the data are analysed in narrow energy ranges, not relying on details of the PSFs; for the catalog, for which a standardised procedure had to be used, a point-source has been postulated and a single wide energy range has been analysed by the likelihood procedure, trusting in the PSF. Thus, the catalog flux does not contain the extended

fraction of the excess (see Fig. 5) and furthermore, part of the flux is attributed to a neighbouring unidentified soft source (see Sect. 3.3).

4. Source scenarios

4.1. Interaction of ambient cosmic-rays with gas

In the GC ($l = 0°$, Sgr A), as near $l = 0.6°$ (Sgr B), $l = 1.2°$ (Sgr D) and $l = 3°$ (Clump 2), there are situated giant molecular cloud complexes. The masses of these complexes are not easily determined and originally had been very much overestimated on the basis of their signal in ^{12}CO-line emission. Blitz et al. (1985) and Stacy et al. (1987) on the basis of the non-detection of a corresponding GC excess in COS-B gamma-ray data have discussed the discrepancy between the ^{12}CO (Dame et al. 1987) tracer prediction and the observed gamma-ray emission from these massive molecular clouds. They already suggested that the ^{12}CO to H_2 conversion factor for these clouds is very much lower than galactic average. These cloud complexes are apparently in an unusual state of high local spherical and turbulent gas velocities (making the ^{12}CO line wide and optically thin), high molecular gas kinetic temperature and increased metallicity. Several authors (Nishimura 1980, Heiligman 1987, Stark et al 1989, Cox & Laureijs 1989, Pajot et al. 1989, Güsten 1989, Lis & Carlstrom 1994, Sodroski et al. 1994, Nakayama et al. 1995) further investigated these clouds on the basis of tracer molecule-line (^{13}CO, CS, C^{18}O) and FIR-(IRAS, COBE-DIRBE, 900 μ) surveys and provide support for reduced mass estimates. Sodroski et al. (1995) conclude that these complexes have 3 to 10 times less mass than originally suggested by the ^{12}CO emission and thus do not dominate the total gas mass in the central 300 pc. The possibility for an even lower gas mass is indicated by CO-line observations of other galaxy-cores by Wall et al. (1989), who find CO/H_2 conversion factors 5 to 20 times lower than our Galaxys average. Stark et al. (1989) suggested that the mass in the NB to a large extent consists of a diffuse molecular inter-cloud medium, only partially bound to clouds.

Even when based on FIR observations, the average diffuse molecular gas surface densities in the NB are still high (≈ 100 H-atoms cm^{-3}, Güsten 1989). However, the NB region is much more evolved compared to the inner Galaxy, the advanced state of astration being reflected by the chemical composition (Wannier 1989). Thus, like the CO to gas, the FIR-emission to dust and the dust to gas conversion factors are subject to uncertainties in this region and are possibly lower than those used in the gas estimate by Cox & Laureijs (1989). It is noted that that the longitude distribution of FIR emission IRAS, COBE-DIRBE) within the NB, in contrast to CO-line distributions, is peaked toward the longitude $l = 0°$ and appears only slightly more extended in longitude than the gamma-ray distribution. However, the absolute amount of gas ($R < 250$ pc) again remains uncertain due to the difficulties in determining the FIR to gas conversion factor in this particular region.

It is emphasized that the gamma-ray data do not show any localized source excesses at the locations of the cloud complexes Sgr B, Sgr C, Sgr D and Clump 2. This finding does not depend on the details of the diffuse model which disregards most of the ^{12}CO emission from these clouds (Bertsch et al., 1993). The non-detection of these complexes also excludes the possibility of a significantly enhanced CR density within these clouds. Further it strongly suggests that the smaller complexes Sgr A and Sgr C (if there is not an enhanced CR density) also do not contribute significantly to the central source excess.

Fig. 5 displays the enclosed-gas-mass estimate based on FIR observations by Cox & Laureijs (1989) depending on galactic radius (dotted line). The corresponding predicted gamma-ray emission > 300 MeV, based on the average emissivity ($1.05\,10^{-26}$ atom^{-1} sr^{-1} s^{-1}) derived for the inner Galaxy < 5 kpc by Strong & Mattox (1995), is indicated by the left-hand scale. Also shown is the EGRET-observed gamma-ray emission: the circle symbol indicates the total flux observed from a volume of 250 pc radius around the GC. For the comparison of the observed gamma-ray emission with the emission expected from the diffuse matter distribution, based on FIR, we use a two-component model (see Sect. 3.2) where an unresolved component ($\sim 60\%$, double-hashed area) originates from within 85 pc and an evidently resolved extended component ($\sim 40\%$, hashed area) is emitted from within 250 pc from the GC. The latter component partially is represented in the diffuse model and partially is observed as an excess exceeding the diffuse model. The observed unresolved gamma-ray source with its peculiar spectrum can well be accommodated when a slightly reduced emissivity ($\sim 11\%$) in the NB relative to the estimate from FIR (Cox & Laureijs,1989) is adopted. This minor difference can as well be attributed to the uncertainties in deriving the gas estimate from FIR as to the uncertainty in the determination of the amount of gamma-ray emission already represented by the diffuse model or to a lower emissivity within this region. Dahmen et al. (1997), on the basis of a detailed analysis of their C^{18}O survey and from ^{12}CO data obtain a somewhat lower value of $\sim 27\,10^6$ solar masses for the volume within 300 pc from the GC.

4.2. Interaction of enhanced cosmic rays with gas or interstellar radiation

The peculiar spectrum of the of the observed gamma-ray emission (Fig. 4), in case of origin from CR-gas interactions, requires a scenario where the CRs, nucleons or electrons, have a very hard and unusual spectrum and where the gamma-ray creation process basically preserves this spectrum. It is difficult to produce the observed hard spectrum from nucleonic interactions, at least for isotropic interaction with the target medium where the 'π^o bump' is always produced. Nothing is known about the nucleonic CR density in the Galactic Bulge, and gamma-rays would be the only tracers. If the gas density increases toward the center and some coupling of CR density to the gas density exists, then the creation of the observed amount of gamma-rays might be feasible; however, the problem of producing the observed peculiar spectrum remains.

Energetic electrons with hard spectra, and subsequent gamma-ray spectra, can more easily be produced. In contrast

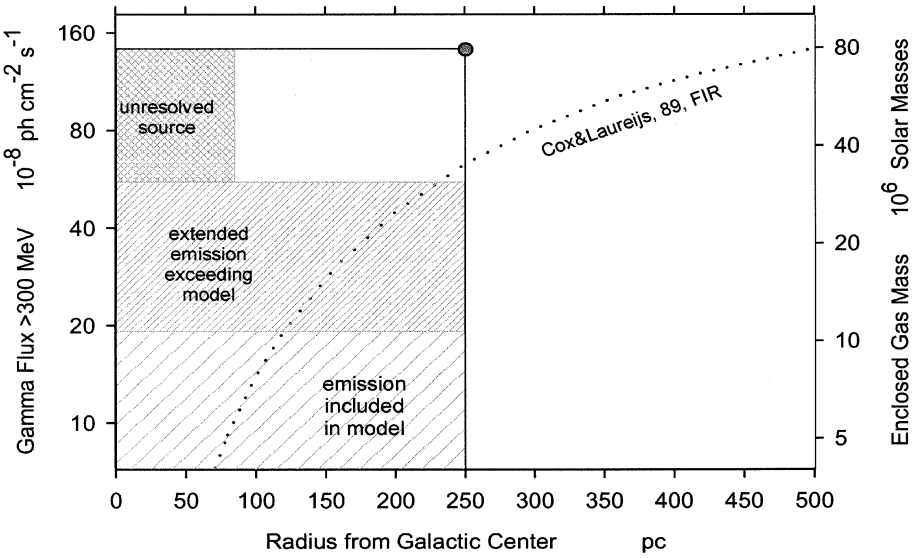

Fig. 5. The spatial distribution of the observed gamma-ray source components are compared with the predicted emission based on the gas estimate from a FIR survey (dotted line) and on the average CR density within a galactocentric radius of 5 kpc. The filled circle gives the total observed flux from within 250 pc around the GC. The hashed areas indicate the components of the total flux: the fraction beeing already represented by the diffuse model, the extended component exceeding the model, and the unresolved source component.

to CR nucleons, high energy electrons are well traced by their non-thermal radio (synchrotron) emission and are indeed observed particularly from the compact source Sgr A* and from the extended radio Arc. Energetic electrons not only can interact via Bremsstrahlung with nucleonic targets, but also can create gamma-rays by inverse-Compton interaction with radiation fields.

The Arc

An appropriate scenario is offered by the radio Arc, where the presence of rather monoenergetic electrons in an extended region is indicated by the observed radio spectrum (Yusef-Zadeh 1989; Lesch & Reich 1992; Pohl et al. 1992; Yusef-Zadeh & Wardle 1993). Pohl (1997) suggests that the electrons, accelerated and confined in the extended flux tube of the Arc, interact with the FIR radiation field originating in a neighbouring massive cloud (M0.20-0.033). This cloud is in contact with the flux tube through an HII region (G0.18-0.04, the 'Sickle'), which also could act as the source injecting electrons into the flux tube. The most energetic of the accelerated electrons can upscatter FIR photons to gamma rays. Pohl's model successfully produces the observed spectrum and intensity.

Sgr A*

The spatial distribution for the interstellar radiation field (star light and FIR reprocessed from dust) near the GC has a HWHM of a fraction of a degree. It peaks sharply within the IRS16 cluster about 1 arcsec west of Sgr A* (Menten et al. 1997), and therefore would provide an appropriate target distribution for the creation of the observed gamma radiation. However, the quasi monoenergetic non-thermal electron spectrum observed from Sgr A* (Duschl & Lesch 1994; Zylka et al. 1995; Beckert et al. 1996; Metzger et al. 1996) is modelled to have a mean energy below 150 MeV and thus is inadequate to produce the observed gamma-ray spectrum.

4.3. Stellar sources

Pulsars

A stellar source or a collection of stellar sources at a distance of 8.5 kpc would need to have a luminosity (> 100 MeV) about equivalent to that of 13 Crab pulsars, 50 Vela Pulsars or 1170 Geminga Pulsars to explain the unresolved fraction of the source excess. As a single source, it would be by far the most luminous source in the Galaxy. Radio emission from young pulsars cannot be detected from the GC region because the dispersion along the line of sight is too great, so the non-detection in radio does not exclude this possibility. From a spectral point of view, the older ($\gg 10^3$ yr) pulsars like Vela or Geminga, provide hard spectra with a break at a few GeV, resembling the observed GC spectrum, while the younger Crab pulsar has a spectrum which is too soft. However, the Crab pulsar is the only example available and one can argue that this single case does not exclude the possibility that other very young pulsars could have a spectrum similar to that of Vela. Thus, disregarding the spectral argument, one or a few very young pulsars could be the sources of the observed emission, provided their individual gamma-ray-emissivity is higher by about an order of magnitude. This could be achieved by an increased breaking energy loss combined with an increased efficiency by which the breaking energy is converted into gamma-ray emission.

It is interesting to consider the alternative case, where the observed luminosity may be produced through an accumulation of many middle-aged pulsars which would provide the observed spectrum. Metzger et al. 1996 conclude that star formation in the NB is not a continuous process, but is rather episodic, possibly recurrent, and that the last mild starburst occurred 10^7 yr ago. Pulsars are suggested to have at birth a kick-off velocity dis-

tribution with a mean velocity of 450 km s^{-1} (Lyne & Lorimer 1994). A fraction of the pulsars evolving from the starbursts in the GC region is ejected with favourable initial velocity vectors (low speed, retrograde ejection) forcing them into low Keplerian orbits around the GC due to the central gravity potential well. This collection of pulsars possibly forms a local (< 1 pc) concentration of sources around the GC which is unique within the Galaxy. However, the number of pulsars which have an age enabling them to emit significant gamma-ray flux appears far too small to make this scenario likely.

Massive black hole

Accretion to the postulated central massive black hole (BH) cannot easily produce the observed gamma radiation. The likely BH of $2.45\,10^6$ solar masses (Eckart & Genzel 1996), postulated to resemble the dark mass located at the GC, which is possibly identical with Sgr A*, apparently is in a 'starving state'. Besides synchrotron radio/IR emission, not much radiation is observed. Sgr A* is only a weak emitter in soft X-rays (Goldwurm et al. 1994) and has never been detected above 30 keV in 6 years of SIGMA data (Vargas et al. 1997). The weak X-ray emission makes it unlikely that the gamma-ray source is related to the wind accretion from the IRS16 cluster to the tentative BH as suggested by Melia (1992) or Mastichiades & Ozernoy (1994). More recently the concept of advection-dominated accretion-flow (ADAF) into BHs has been suggested (Mahadevan et al. 1997). Markoff, Melia and Sarcevic (1997) performed a refined calculation of the particle cascade and explain the observed spectrum to some extent by a combination of proton-synchrotron radiation and pion decay. However, the emission in the high-energy gamma-ray regime in all models is dominated by pion-production and – decay and therefore the models do not easily produce the very hard spectrum with its sharp turnover, which is observed for the GC source. Clearly emission in the vicinity of a supermassive BH remains a possibility; however its feasibility still is not convincingly demonstrated.

4.4. Other scenarios

Dark matter

The 'neutralino' species of the WIMPs (weak interacting massive particles) are the lightest particles within the SUSY model of particle physics and are expected to concentrate in the centers of galaxies forming non-dissipative gravitational singularities (NGS). These gravitational potential wells may act as seeds for generating massive BHs. The sharp increase in neutralino density near the singularity leads to neutralino annihilation, which might be traced by decay products including gamma rays in the MeV to TeV range (Silk & Bloemen 1987, Stecker & Tylka 1989; Berezinsky et al. 1992; Urban et al. 1992). The spectra expected from annihilation of neutralinos, particularly of photinos, higgsinos, etc. in the GC consist of a flat continuum in the range above 100 MeV, dropping exponentially at several GeV, and also containing a line corresponding to the neutralino mass; possible values for the neutralino mass range from 5 GeV to several 100 GeV. Stecker & Tylka (1989) obtain for a neutralino mass of 15 GeV a spectrum which is compatible with the observed GC source spectrum. They use the isothermal model for the dark-matter-core by Ipser and Sikivie (1987), which provides a central core density distribution compatible with the observed source, and predict a gamma-ray intensity which is a factor 4 less than observed. This difference can be considered small with respect to the available freedom in the choice of model parameters. However, Berezinsky et al. 1992, on the basis of the radio emission expected from electrons, which also emerge from the decay processes, argue for a lower neutralino mass limit of > 150 GeV yielding much lower intensities in the GeV range. So the possibility that the GC source represents neutralino decay remains speculative; the safest indication that such processes are actually occuring within the NB could come from the detection of the accompanying neutralino annihilation-line which is expected within the energy range from 10 GeV to a few 100 GeV.

5. Summary

A strong high-energy gamma-ray excess, on top of the expected galactic diffuse emission is observed to originate from a volume of typically 85 pc or 0.6 degree radius peaking within 30 pc or 0.2 degrees from the actual GC. The emission volume is likely extended or contains multiple sources; however, it is still marginally compatible with a point source. The observation is well described by an unresolved emission peak, located on top of an extended (resolved) emission excess which represents about 40% of the total flux emitted from the volume with radius 250 pc around the GC; the latter extended component could represent the diffuse emission expected from interaction of interstellar gas and inner-galactic average-density Cosmic Rays. The source flux appears to be stable over the EGRET observation epochs: some indication for short term variation within a factor of 2 exists, but this apparent variation is more likely due to systematic uncertainties in the measurement. A reanalysis of the earlier COS-B data showed that the intensity observed by COS-B from the GC is compatible with that observed by EGRET. The spectrum is very hard up to 2 GeV, where it turns over sharply; thus it is distinctly different from the spectrum of the large-scale galactic diffuse emission, within which the GC source is embedded.

The earlier finding that the non-detection by COS-B of a prominent gamma-ray source at the GC requires lower masses for the molecular cloud complexes in the NB than indicated by naive interpretation of other gas tracers is confirmed, in spite of the detection of the strong GC source excess by EGRET. However, this confirmation is now based on the longitude distribution, which does not trace the cloud complexes seen in CO, and on the peculiar spectrum of the observed emission. The total gas mass within 250 pc from the GC derived in this analysis is found to be compatible with the estimates from FIR surveys.

For the central unresolved source excess, based on the observed peculiar spectrum, on the limited extent of the source and

on the apparent lack of time variation, three different source scenarios are favoured candidates: A single or a few very young pulsars (< 1000 yr), which would need both a high rate of energy loss and a very high gamma-ray emission efficiency, could produce the observed source excess, equivalent to the emission of ~ 13 Crab pulsars. This scenario postulates that the observed spectrum of the Crab pulsar is not representative for the spectral properties of very young pulsars.

Radio spectra indicate the presence of high-energy quasi-monoenergetic electrons in the flux tube of the radio Arc structure near the GC. These electrons interact with the FIR radiation field of the neighbouring massive molecular cloud and could emit gamma-rays by inverse-Compton boosting of the FIR photons, providing a compact gamma-ray source with the observed spectrum and intensity.

WIMPs are hypothesised to concentrate in the center of the galaxy-forming dark-matter cores with densities high enough to trigger neutralino annihilation. The annihilation processes produce, through several decay channels, gamma rays with a continuum spectrum above 100 MeV and an annihilation line corresponding to the neutralino mass. The spectrum and expected intensity depends strongly on the neutralino mass, which is unknown. The source extent is expected to be compatible with the observation for a wide range of core-model parameters.

To proceed significantly further, new observations in the 100 MeV to 100 GeV regime, with higher spatial resolution and higher sensitivity, are required aiming to determine better the extent and possible time variation of the source and the high-energy continuation of the spectrum. This task will have to await a next-generation high-energy instrument such as GLAST. Earlier progress might arise from the atmospheric Cerenkov telescopes sensitive below 1 TeV just becoming operational or under construction; however, the steep spectral decrease of the spectrum above 2 GeV might inhibit the detection.

Acknowledgements. The EGRET team gratefully acknowledges support from the following: Bundesministerium für Bildung, Wissenschaft, Forschung, und Technologie (BMBF), Grant 50 QV 9095 (MPE authors), NASA Grant NAG 5-1742 (HSC); NASA Grant NAG-1605 (SU); and NASA Contract NAS 5-31210 (GAC). We thank Isbelle Greiner for helpful comments.

References

Beckert, T., et al. 1996, A&A 307, 450
Berezinsky, V.S., Gurevich, A.V. and Zybin, K.P. 1992, Phys.Lett. B294, 221
Bertsch, D.L., et al. 1993, ApJ 416, 587
Blitz, L., et. al. 1985, A&A 143, 267
Cox P. & Laureijs, R. 1989: The Center of the Galaxy, ed. M. Morris, Kluwer, Dordrecht, IAU Symp. 136, pp. 121
Dahmen G., et al. 1997, A&AS 126, 197
Dame T.M., et al. 1987, ApJ 322, 706
Duschl, W.J. & Lesch, H. 1994, A&A 286, 431
Eckart, A., et al. 1993, ApJ 407, L77
Eckart, A. & Genzel, R. 1996, Nature 383, 415
Esposito, J.A. 1998, in preparation
Fierro, J.M. 1995: Observ. of Spin-Powered pulsars with EGRET, Thesis, Stanford University
Genzel, R. and Townes, C.H. 1987, ARA&A 25, 377
Güsten, R. 1989: The Center of the Galaxy, ed. M. Morris, Kluwer, Dordrecht, IAU Symp. 136, pp. 89
Goldwurm, S.A., et al. 1994, Nature 371, 589
Heiligman, G. 1987, ApJ 314, 747
Hartmann, R.C., et al. 1998, ApJS, in preparation
Hermsen, W. 1980, Gamma-Ray Sources, Thesis, Rijksuniversiteit Leiden
Hunter, S.D., et al. 1994, ApJ 436, 216
Hunter, S.D., et al. 1995: Proc. 24th ICRC 2, 182
Hunter, S.D., et al. 1997, ApJ, in press
Ipser, J.R. & Sikivie, P. 1987, Phys. Rev. D35, 3695
Krichbaum, T.P., et al. 1993, A&A 274, L37
Lamb, R.C. & Macomb,D.J. 1997, ApJ 448, 872
Lesch, H. & Reich, W. 1992, A&A 264, 493
Lis, D.C. & Carlstrom, J.E. 1994, ApJ 424, 189
Lyne, A.G. & Lorimer, D.R. 1994, Nat 369, 127
Mahadevan, R., Narayan, R., Krolik, J. 1997, ApJ 486, 268
Markoff, S., Melia, F., Sarcevic, I. 1997, ApJ 489, L47
Mastichiadis, A. & Ozernoy, L.M. 1994, ApJ 426, 599
Mayer-Hasselwander, H.A., et al. 1982, A&A 105, 164
Mayer-Hasselwander, H.A. 1992: Talk given at First Compton Symposium, St. Louis
Mayer-Hasselwander, H.A. 1993: Proc. 23rd ICRC, Calgary, 1, pp. 47
Mattox, J.R. 1996, ApJ 461, 396
Melia, F. 1992, ApJ 387, L25
Menten, K.M., et al. 1997, ApJ 475, L111
Merck, M., et al. 1996, A&AS 120, 465
Mezger, P.G., et al. 1996, A&AR 7, 289
Nakagawa, T., et al. 1995, ApJ 455, L35
Nishimura, T., et al. 1980, ApJ 239, L101
Pajot, F., et al. 1989, A&A 223, 107
Pohl, M., et al. 1992, A&A 262, 441
Pohl, M. 1997, A&A 317, 441
Reimer, O., Dingus, B.L., Nolan, P.L. 1997, Proc. $25^{\rm th}$ ICRC, Durban, 3, pp 97
Silk,J., Bloemen H. 1987, ApJ 313, L47
Sodroski, T.J., et al. 1994, ApJ 428, 638
Sodroski, T.J., et al. 1995, ApJ 452, 262
Sreekumar, P. 1997: Proc. $4^{\rm th}$ Compton Symposium, Williamsburg
Stark, A.A., et al. 1989, The Center of the Galaxy, ed. M. Morris, Kluwer, Dordrecht, IAU Symp. 136, pp. 129
Stacy, J.G., et al. 1987, Proc. 20th ICRC, 1, 17
Stark, A.A., et al. 1991, MNRAS 248, 4
Stecker, F.W. & Tylka, A.J. 1989, ApJ 343, 169
Strong, A.W. 1996, Space Science Rev. 76, 205
Strong, A.W. & Mattox, J.R. 1996, A&A 308, L21
Thompson, D.J., et al. 1995, ApJS 101, 259
Urban, M., et al. 1992, Phys. Lett. B 293, 149
Yusef-Zadeh, F. 1989, The Center of the Galaxy, ed. M. Morris, Kluwer, Dordrecht, IAU Symp. 136, pp. 243
Yusef-Zadeh, F. & Wardle, M. 1993, ApJ 405, 584
Vargas M., et al. 1997, ApJ 476, L23
Wall, W.F., et al. 1993, ApJ 414, 98
Wannier, P.G. 1989, The Center of the Galaxy, ed. M. Morris, Kluwer, Dordrecht, IAU Symp. 136, pp. 107
Zylka, R., et al. 1995, A&A 297, 93